

INTEGRATED THERMAL ANALYSIS OF THE FRIB CRYOMODULE DESIGN*

Y. Xu[#], M. Barrios, F. Casagrande, M. Johnson, M. Leitner, FRIB, East Lansing, MI 48824, USA
D. Arenius, V. Ganni, W.J. Schneider, M.A. Wiseman, Jefferson Lab, Newport News, VA 23606, USA

Abstract

Thermal analysis of the FRIB cryomodule design is performed to determine the heat load to the cryogenic plant, to minimize the cryogenic plant load, to simulate thermal shield cool down as well as to determine the pressure relief sizes for failure conditions. Static and dynamic heat loads of the cryomodules are calculated and the optimal shield temperature is determined to minimize the cryogenic plant load. Integrated structural and thermal simulations of the 1100-O aluminium thermal shield are performed to determine the desired cool down rate to control the temperature profile on the thermal shield and to minimize thermal expansion displacements during the cool down. Pressure relief sizing calculations for the SRF helium containers, solenoids, helium distribution piping, and vacuum vessels are also described.

INTRODUCTION

There are four primary configurations of cryomodules to be built for FRIB: 80.5 MHz $\beta=0.041$, 80.5 MHz $\beta=0.085$, 322 MHz $\beta=0.29$ and 322 MHz $\beta=0.53$. The detailed FRIB cryomodule design is provided in [1] of this proceeding.

Simulation and analysis are important to guide and verify the cryomodule design, which includes design of cold mass, cryogenic, thermal radiation shield, magnetic shield, and vacuum vessel sub-systems. The thermal simulations and analysis involved in designing a cryomodule include the heat load calculation; cool down simulation of thermal shield, solenoids and resonators; pressure relief calculation of helium and vacuum system; flow calculation of cryogenic sub-system to determine the pressure, temperature and mass flow rate of helium.

In this paper, the heat load calculation, thermal shield simulations and pressure relief calculation will be presented.

HEAT LOAD

The static heat load contribution includes conduction through cryomodule supports, fundamental power couplers (FPCs), tuners, pressure relief pipes, beam line pipes, valves, magnet power supply leads, instrumentation wires and helium system bayonets, and radiation to shields and cold mass.

The dynamic heat load contributions are from ohmic heating of the power couplers and RF losses in the resonators. Details of the heat load calculation are documented in FRIB report [2].

Static and Dynamic Heat Loads

The inverse Coefficient of Performance (COP_{inv}) states how many watts of input power are required to produce one watt of cooling power. The ideal COP_{inv} is given in Table 1 and is normalized such that at 4.5 K the ideal COP_{inv} is 1 for convenience. In reality, more watts of input power are required to produce one watt of cooling power in 2 K. Hence, the coefficient at 2 K is 3. The 4.5 K normalized cryogenic plant load is therefore calculated by

$$q = 3q_{2k} + q_{4.5K} + 0.1q_{40K}$$

Table 1: Coefficient of Performance

| Circuit Temperature [K] | COP | COP_{inv} [W/W] | 4.5 K Norm. [W/W] |
|-------------------------|--------|-------------------|-------------------|
| 2 | 0.67% | 149 | 3 |
| 4.5 | 1.52% | 65.7 | 1 |
| 40 | 15.38% | 6.5 | 0.1 |

The calculated cryomodule heat loads are given in Table 2. The components with conduction paths are intercepted with a thermosyphon loop supplied by a liquid helium bath at 4.5 K and a gaseous 40 K helium supply. Locations of the intercepts are calculated to minimize the cryogenic plant load. Temperature of the intercepts considers the thermal resistivity from the intercepts to the 4.5 K and 40 K cryogenic circuits and the heat loads to the circuits.

Table 2: Cryomodule Static and Dynamic Heat Loads

| Heat Load [W] | $\beta=0.041$ (4 cavities) | $\beta=0.085$ (8 cavities) | $\beta=0.29$ (6 cavities) | $\beta=0.53$ (8 cavities) | |
|---------------|-------------------------------|-------------------------------|------------------------------|------------------------------|-------|
| 2 K | Static | 4.6 | 8.2 | 6.8 | 9.7 |
| | Dynamic | 5.8 | 32.1 | 22.6 | 65.2 |
| 4.5 K | Static | 15.7 | 25.8 | 17.0 | 20.9 |
| | Dynamic | 2.7 | 7.1 | 7.3 | 12.8 |
| 40 K | Static | 120.8 | 141.8 | 129.5 | 139.7 |
| | Dynamic | 4.0 | 11.2 | 12.2 | 22.1 |
| Total | | | | | |
| 2 K | 10.4 | 40.3 | 29.4 | 74.9 | |
| 4.5 K | 18.4 | 32.9 | 24.3 | 33.7 | |
| 40 K | 124.8 | 153.0 | 141.7 | 161.8 | |

*Work supported by US DOE Cooperative Agreement DE-SC0000661
#xut@frib.msu.edu

Optimal Shield Temperature

To obtain the optimal shield temperature, different thermal shield temperatures ranging from 20 K to 60 K are compared in Figure 1. To make a rational comparison, heat loads at 2 K and 40 K are converted to a normalized 4.5 K load.

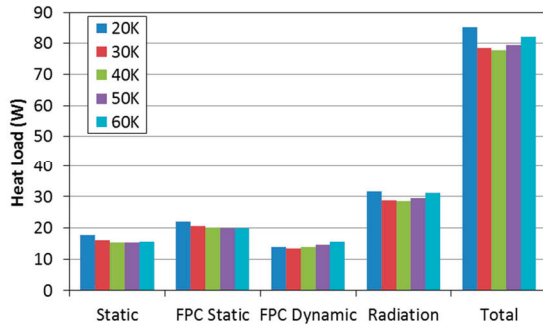


Figure 1: Heat load for different shield temperatures.

Static heat load includes conduction through components, radiation of beam line flanges and pressure relief devices, and helium conduction and convection inside pressure relief pipes. Radiation heat load is reduced using multilayer aluminized mylar insulation (MLI). A 30 layer blanket is used on the 40 K thermal shield and 10 layers on the 2 K and 4.5 K mass. The radiation heat fluxes are 3 W/m² from 300 K to 40 K shield and 0.4 W/m² from 40 K shield to cold mass under vacuum of 10⁻⁵ torr, respectively. FPC static heat load calculations include conduction through the outer conductor and radiation from the inner conductor. FPC dynamic load includes additional resistive heat input. The dynamic heat load from the resonators is 63.2 W at 2 K, which does not change with the shield temperature, and hence is not shown in Figure 1. When the shield temperature is 40 K, total heat load of the cryomodule reaches the minimum.

THERMAL SHIELD COOL DOWN

For manufacturing and assembly considerations, the thermal shield is composed of three sections. The shield is cooled via parallel 12.7 mm helium cooling tubes welded to the 1100-O aluminium sheet.

Cool Down Rate

Simulation of the thermal shield is performed for 40 K 3 atm helium gas for mass flow rates of 0.1, 0.3, 1 and 3 g/s. The corresponding heat transfer coefficients are 38, 92, 240 and 580 W/m²·K, respectively. The change of temperature gradient on the shield with time is shown in Figure 2. The larger the helium mass flow rate, the faster the cool down rate. For example, temperature on the thermal shield reaches steady state within 1.7 hours with 3 g/s mass flow rate, while it takes 2.2 hours for 1 g/s, 3.2 hours for 0.3 g/s and 5 hours for 0.1 g/s.

Temperature profile at the steady state is displayed in Figure 3. The minimum temperature is 41.6 K, while the maximum is 43.8 K and occurs in the vertical plane where the heat conduction path is the greatest.

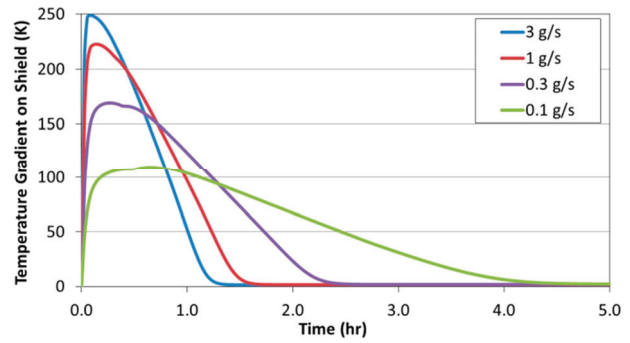


Figure 2: Cool down rate for different mass flow rates.

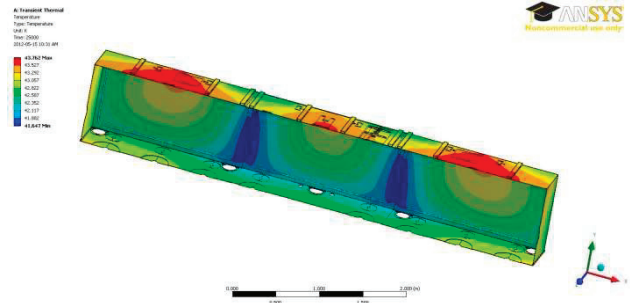


Figure 3: Temperature profile on thermal shield (half).

Deformation

The maximum displacement of the shield is 6.1 mm after 3.3 hrs as shown in Figure 4. The shield is supported from below on composite links. During cool down the shield displacements are minimized by the division into one third of the overall length. Each section of the shield shrinks toward its geometric center. The three shield sections have 16 mm overlap providing shielding through cool down. The thermal stress analysis during cool down is ongoing to determine the maximum cool down rate that the shield can accept.

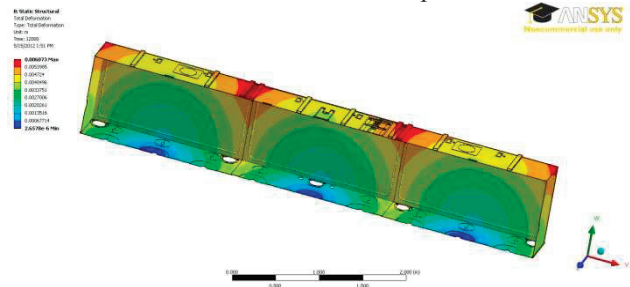


Figure 4: Thermal shield deformation.

PRESSURE RELIEF SIZING

Four pressure relief sizing calculations are presented in this paper: vacuum vessel, 2 K circuit, 4.5 K circuit and helium pipes. The pressure setting and boundary conditions for the calculations follow the guidelines of ASME code [3] and CGA S-1.3 2008 [4]. The calculation of the relief size implements the basic fluid dynamics rules and obeys the first and second thermodynamic laws. Details of the pressure relief sizing calculation and the safety handling are documented in FRIB report [5].

Failure Modes

Potential failure modes and the corresponding pressure relief devices (PRDs) to protect the system are listed in Table 3.

The heat transfer process involved in the pressure relief sizing calculation is very complicate. Hence, the determination of heat flux contributed to the gas expansion is difficult. Experiments have been performed for different cryostats under different failure modes to determine the heat flux [6]-[10], which varies from 1.5 kW/m² to 40 kW/m². The heat fluxes adopted in the calculation for FRIB cryomodules are the most conservative values from the literatures.

Table 3: Failure Modes and Pressure Relief Devices

| Failure Mode | Causes | Heat Flux [kW/m ²] | Pressure Relief Devices |
|-------------------------------------|---|--------------------------------|---------------------------------|
| Loss of beam line vacuum to air | Diagnostic box venting | 40.0 | Parallel plate |
| | Failure of power coupler bellow FPC ceramic window break | | |
| Loss of insulation vacuum to air | Tuner bellow vacuum failure | 6.0 | Parallel plate; Relief valve |
| | Power coupler vacuum failure | | |
| | Vacuum vessel leak | | |
| Loss of insulation vacuum to helium | Helium vessel leak | 1.5 | Parallel plate; Relief valve |
| | Helium pipe leak | | |
| Solenoid quench | | | Parallel plate |
| Helium gas increase | Return valve close | | Relief valve |

2 K Cryogenic Circuit Pressure Relief

For resonator helium vessel relief, the worst case scenario is loss of beam line vacuum to air. The pressure in the helium vessel when the PRD activates is given in Figure 5 for different relief pipe inner diameters. The resonator's yield pressure under cryogenic condition is 15 atm. A cryogenic maximum allowable working pressure (MAWP) of 10 atm has been chosen. Therefore, a 2" IPS Schedule 5 pipe (inner diameter 5.7 cm) will be used as the relief pipe. The set pressure of the PRD is 11 atm.

4.5 K Cryogenic Circuit Relief

The worst case scenario of the 4.5 K cryogenic circuit pressure relief occurs during solenoid quench. When a solenoid quenches, the 90 KJ stored energy will be absorbed by the cold mass and liquid helium residing in the solenoid and header, occurring in a short duration. A conservative assumption is made that the 90 kJ of stored energy is absorbed by helium in 2 seconds. The pressure at the solenoid when the PRD activates is given in Figure

5 for different relief pipe inner diameters. Therefore, a 1" IPS Schedule 5 pipe (inner diameter 2.7 cm) will be used as the relief pipe. The set pressure of the PRD is 5 atm.

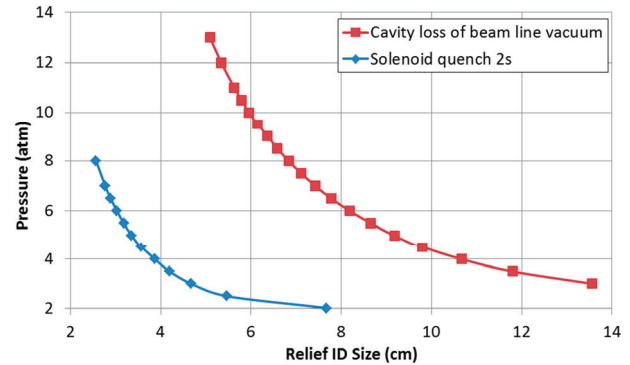


Figure 5: Pressure in helium vessel vs. relief pipe size.

Vacuum Vessel Relief

The vacuum vessel shall be protected by a suitable pressure relief device such that it is not a pressure vessel. The minimum relief area is determined by the larger value of the discharge area of vacuum jacket required by [4] and the minimum helium relief area when cryogen lines in cryomodule rupture.

The minimum discharge area of vacuum jacket required by [4] is 24 cm² given a vacuum vessel volume of 7 m³. When helium pipes rupture, the maximum mass flow rate is 458 g/s. To release this amount of helium to room temperature, the minimum relief area is 223 cm². Hence, the minimum relief pipe size for vacuum vessel is 16.5 cm.

Helium Piping Relief

Pressure relief devices are required for the helium piping between two adjacent valves for the failure case of a closed return valve for both thermal shield and cold mass helium pipes. The PRDs require a flow capacity greater than 29 and 12 SCFM air at room temperature of thermal shield and cold mass helium pipes relief, respectively. Therefore, 0.635 cm relief valves with set pressure of 3.7 atm are sufficient.

REFERENCES

- [1] M. Johnson et al., "Design of FRIB Cryomodule," WEPPD006, this proceeding.
- [2] FRIB report T30802-EN-000004, unpublished.
- [3] ASME Boiler and Pressure Vessel Code Section VIII – Rules for Construction of Pressure Vessels.
- [4] CGA S-1.3, 2008.
- [5] FRIB report T30802-EN-000003, unpublished.
- [6] W. Lehman and G. Zahn, ICEC7, London, 1978, pg. 569.
- [7] M. Wiseman et al., *Advances in Cryogenic Engineering*, Vol. 39, 1994, pg. 997.
- [8] G. Cavallari et al., *4th Workshop on RF Superconductivity*, Japan, August 14-18, 1989, SRF89G28, pg. 781.
- [9] T. Boechmann et al., "Experimental Test of Fault Conditions during the Cryogenic Operation of a XFEL Prototype Cryomodule," ICEC-ICMC 2008.
- [10] M. Wiseman et al., *Applications of Cryogenic Technology*, Vol. 10, 1991, pp. 287-303.